

ELECTRIC CONTROL DESIGN AND STABILITY TEST ANALYSIS OF HYDRAULIC FOUR-WHEEL DRIVE CHASSIS

Ying LV, Manfeng GONG, Guangbin WANG*

An electro-hydraulic control system is adopted to control the electromagnetic reversing valve of the swing steering motors to realize front wheel steering. When one side of the reversing valve oil circuit is open and the other is closed, the speed between the left and right traveling wheels will be different. The electro-hydraulic control system is established and experimentally evaluated by the relay contact electrical scheme. In the test, the chassis was easy to operate and the shifting lever can be used to realize straight moving and steering of the chassis. The results showed that the chassis can achieve high straightness on smooth road surfaces with a deviation rate of less than 1% even without any rider. There is a linear relationship between the minimum deflection angle and the speed of the chassis, and the straight-line and steering trajectories of the chassis is presented by the watermark method. The pressure test on each motor of the chassis showed that when driving straight, the pressure difference between motors was controlled at (within) 0.6Mpa, and the pressure change was also within the allowable range. The chassis runs stably.

Keywords: Four-wheel drive chassis; swing-steering type; electrical control; experimental investigation

1. Introduction

In southern China, there are many small irregular paddy fields. The existing small-scale agricultural machinery cannot meet the automation requirements of small plots, which limits the mechanization level of small plot paddy fields [1-3]. Currently, small crawler tractors are mainly used for harvesting; walking tractors are used for raking, and four-wheel steering tractors are used for transporting rice seedlings in paddy fields [4-6]. However, in addition to the convenient steering of walking tractors, the deflection and steering of four-wheel tractors require a larger field width, which has a great impact on the working efficiency [7-8]. Therefore, the steering sensitivity and stability of the chassis are the most important to realize the mechanization. In order to improve the stability and maneuverability of paddy field four-wheel chassis, it is of great theoretical and practical significance to study a front axle swing-steering

*Department of Mechatronic Engineering, Institute of Mechanical and Electrical Engineering, Lingnan Normal University, Guangdong, Zhanjiang, China
E-mail: jxxwgb@lingnan.edu.cn

four-wheel chassis with better steering characteristics to promote the mechanization of agriculture.

2. Principle of the front axle swing-steering chassis

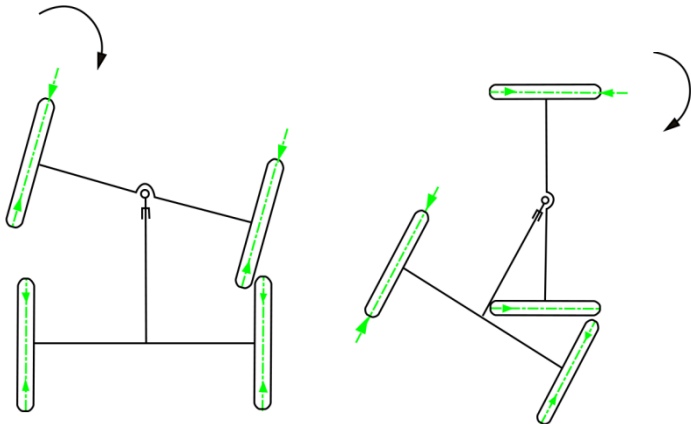


Fig. 1 Diagram of chassis steering force

The front axle swing-steering chassis can realize the overall steering by controlling the walking wheel on one side, so as to achieve the flexible steering characteristics and small turning radius on small paddy fields. It makes the front axle actively swing around the stalled driving wheel at a large angle, and drives the rear axle to steer. As such, it has higher maneuverability than traditional tractors. Besides, the larger the deflection angles of the front axle, the easier the center of the front axle to rotate to reduce the steering resistance moment. As shown in Fig.1, the front axle swing four-wheel drive chassis in this paper adopts the electro-hydraulic control mode. According to the dynamic model of the straight-line driving and steering of the chassis, an electric control system matching with the chassis is established. The electro-hydraulic stability of the chassis during the straight driving and steering is experimentally analyzed, and the results provide a theoretical basis for the optimization of the follow-up control system.

The angular velocity of each wheel of the front axle swing chassis is constantly changing, and its steering dynamics can be analyzed based on its movement. During the motion analysis, segment processing can be performed. When the steering angle is in the range of 0° - 85° , the right rear wheel always moves forward, and the direction of resistance is opposite to that of movement. When the rotation angle is in the range of 90° - 180° , the right rear wheel always moves backward, and the direction of resistance is opposite to that of movement. Furthermore, when the right rear wheel moves from 85° to 90° , it is affected by the resistance torque and sliding friction resistance of the hydraulic motor.

At a rotation angle of 0°-110°, the angular velocity of the left front wheel of the front axle swing chassis is larger than that of the left rear wheel. When steering, the rear axle has no effect on the rotation of the left front wheel around the right front wheel. As such, the steering force only consists of the driving force given by the engine.

At a rotation angle of 110°-180°, the angular velocity of the left front wheel of the front axle swing chassis is smaller than that of the left rear wheel. In this special state, the speed change between the two wheels can be adjusted to ensure the mechanism is not damaged.

When the rotation angle of the front axle is between 0° and 85°, the right front wheel of the front axle stops rotating. All the power of the chassis is transmitted to the left front wheel, and the right rear wheel follows the forward direction. The driving torque of the wheel is caused by the driving force. From the formula it can be concluded that as the front axle angle changes, the resistance of the chassis becomes large. The resistance is at its maximum when the steering is initially achieved and decreases as the angle changes. The specific mathematical model of the steering moment for the whole machine is as follows:

$$M_{zq} = \frac{B}{2} P_{zq} = \frac{Bpq\eta_m}{4\pi r} \quad (1)$$

The total steering moment is as follows:

$$M_{\Sigma} = M_{zhf} + M_{yhf} + M_{zqf} + M_{yqf} = fm_1g \frac{B}{2} \cos \alpha + \mu m_2g \frac{B}{2} \cos \alpha + \mu(m_3 + m_4)g \sqrt{L^2 + \frac{B^2}{4}} \cos \beta \quad (2)$$

$$M_z = M_{zh} + M_{zq} = \frac{B}{2} P_{zq} \cos \alpha + \sqrt{L^2 + \frac{B^2}{4}} P_{zh} \cos \beta \quad (3)$$

where, M_{yqf} , M_{zqf} , M_{zhf} , and M_{yhf} are the steering resistance moments of the right front wheel, the left front wheel, the left rear wheel and the right rear wheel, respectively; P_{zq} , P_{zh} , and P_{yh} are the driving forces of the left front wheel, the right rear wheel and the right rear wheel, respectively; f and μ are the coefficients of the sliding friction and the rolling friction, respectively; L is the wheel track; B is the wheel base; α is the angle between the front axle and the horizontal plane; β is the angle between the rear axle and the horizontal plane; m_1 , m_2 , m_3 and m_4 are the masses of the right front wheel, the left front wheel (Kg), the left rear wheel (Kg) and the right rear wheel, respectively.

$$\begin{aligned} M_{\Sigma} &= M_{zhf} + M_{yhf} + M_{zqf} + M_{yqf} \\ &= fm_1g \frac{B}{2} \cos \alpha + \mu m_2g \frac{B}{2} \cos \alpha + \mu(m_3 + m_4)g \sqrt{L^2 + \frac{B^2}{4}} \cos \beta \end{aligned} \quad (4)$$

The balance torque equation before the front axle of the chassis rotates 85° is as follows:

$$\begin{aligned}
 M_z &= M_\Sigma \\
 \frac{B}{2} P_{zq} \cos \alpha + \sqrt{L^2 + \frac{B^2}{4}} P_{zh} \cos \beta \\
 &= fm_1 g \frac{B}{2} \cos \alpha + \mu m_2 g \frac{B}{2} \cos \alpha + \mu(m_3 + m_4) g \sqrt{L^2 + \frac{B^2}{4}} \cos \beta
 \end{aligned} \tag{5}$$

3. Optimization design of the electro-hydraulic control circuit of the chassis

According to the mechanical analysis of the chassis [9-11], it can be concluded that during the steering process, the torque required for paddy field is relatively large due to the operation and working state of the chassis. Considering the realization of automatic chassis control, the chassis adopts the electro-hydraulic coordination control system, water cooling system, CVT (Continuously Variable Transmission) continuously variable gasoline engine and storage battery, and the output voltage is 12 V [12-13]. The control block diagram of the hydraulic system is shown in Fig. 2. The electrical control and the engine adopts the same power supply, with a 12-V storage battery, and a 220-V AC (Alternating current) solenoid valve is used as the control valve of the hydraulic system [14-15]. The electrical control scheme is shown in Fig. 2. The battery converts the direct current (DC) signal into an alternating current signal through the inverter to supply power to the electrical system, ensuring the driving, PTO (power take-off) and lifting of the hydraulic system.

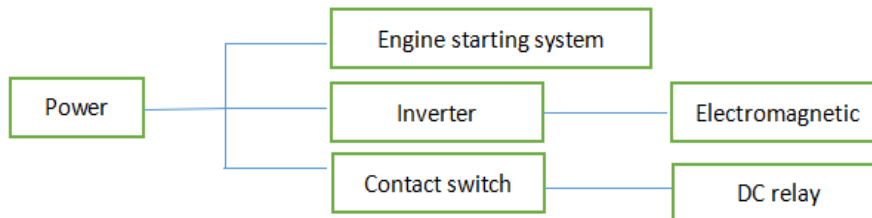
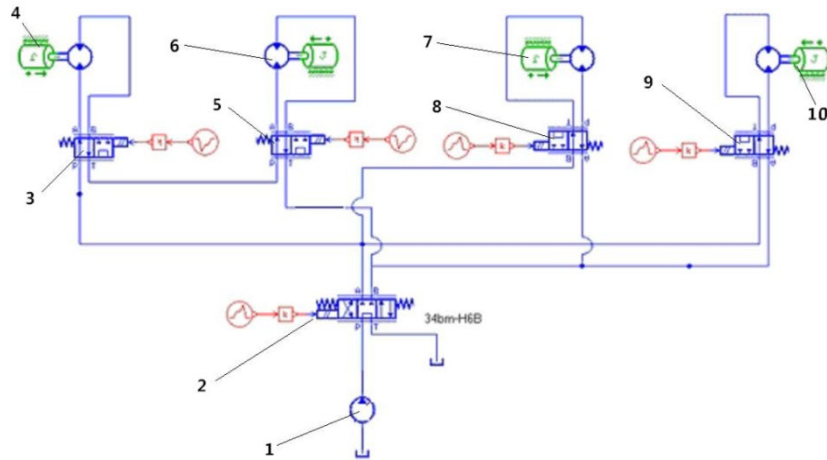


Fig. 2 Electrohydraulic control block diagram

The control method of the hydraulic system swing-steering chassis is special. The electromagnet has a short suction time and adopts wet AC [15-17]. To achieve automatic control of the chassis in a practical design, a directional valve is required to control the on/off state of the liquid flow into the actuator or to change the direction of the oil. The directional control valve can realize the start-stop of the chassis drive system, the conversion of the drive mode, the

start-stop of the PTO system, and the fast walking switching system. The electro-hydraulic control system has six solenoid valves and eight action magnets, and adopts a relay-contact electrical control scheme. The electrical control system has a reversing circuit, a flow control circuit, and a lifting position locking circuit.



1. Oil pump 2. Three-position four-way valve 4, 6, 7, 10. Hydraulic motor. 3, 5, 8, 9 two-way valve
Fig.3 Chassis hydraulic control system

In order to meet the changing trend of the angular velocity between the walking wheels when the chassis turns. Four identical hydraulic motors are used to drive four walking wheels. The hydraulic motors of the two front wheels are connected in series, and then the hydraulic motors of the two rear wheels are connected in parallel. The two front wheel hydraulic motors are connected in series to ensure that the four-wheel chassis can realize straight line walking, and the three lines are connected in parallel to meet the requirements of angular velocity change and time difference of each wheel in the steering process. One shaft and two pumps are used to drive the walking wheel and the power output shaft respectively, which is conducive to the matching of the power output shaft and the walking speed parameters, and the two pumps are used to drive the walking wheel to achieve fast walking when the power output shaft is not needed. As shown in Fig. 3.

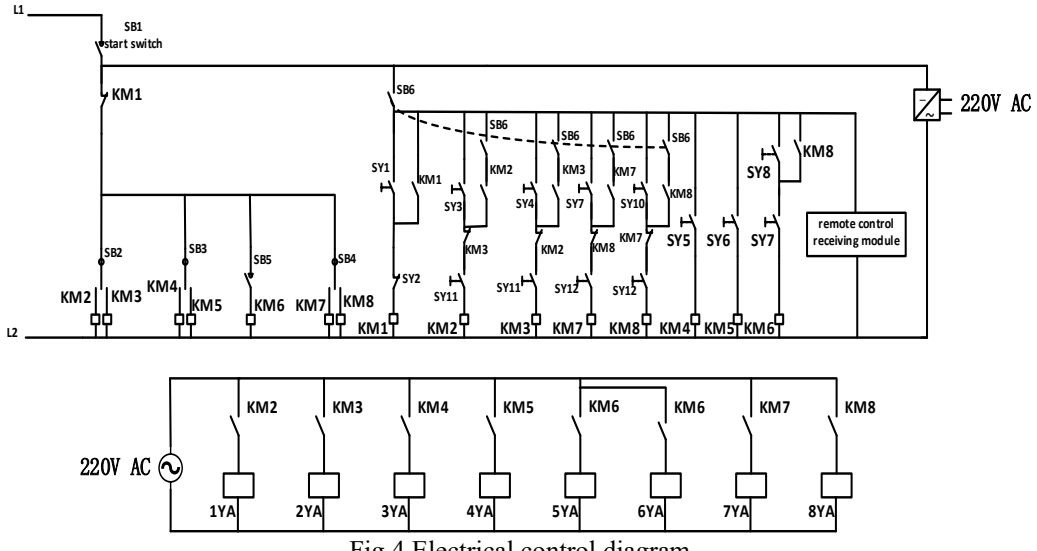


Fig.4 Electrical control diagram

The electromagnet of the directional control valve in the hydraulic system is shown in Fig.4. The electromagnets 1YA and 2YA control the straight-line travel, backward travel and stop of the chassis traveling system. The electromagnets 3YA and 4YA control the steering of the chassis; 5YA and 6YA control the driving mode, and 7YA and 8YA control the start-stop of the PTO output system and the fast walking system. The operating relationship between the chassis and the solenoid valve is given in Table 1.

The relationship between the chassis state and the solenoid valve is displayed in Fig.4, where SB1 denotes the main switch of the control system. The normally closed electric shock of KM1 is connected in series with the manual rocker switch group. When SB6 and SY1 are closed, the normally closed contact of KM1 (contacto) is opened, and the normally open contact is closed. At this time, the manual rocker switch group is power off; the manual control is invalid, and the wireless remote control keeps working. In this way, the chassis can always only work in one control mode, i.e., the manual control and the remote control form an interlocked state, which can prevent possible misoperations when these two control modes are parallel. After SB1 (SwitchButton) is closed, the inverter is always in the working mode, which can convert the input 12-V DC current signal into a 220-V sine wave AC signal. When the corresponding relay is power-on or power-off, the corresponding solenoid valve will be on working to realize the chassis control.

Table 1

Action	State of the chassis and the solenoid valve								
	Working state of electromagnet(+power supply,-power off,attonity)	1YA	2YA	3YA	4YA	5YA	6YA	7YA	8YA
FWD-FWD-forward wheel drive		/	/	/	/	+	+	/	/
FWD-forward wheel drive		/	/	/	/	-	-	/	/
Four-wheel drive		/	/	/	/	/	/	/	/
Go forward		+	-	/	/	/	/	/	/
Turn back		-	+	/	/	/	/	/	/
Turn left		/	/	-	+	/	/	/	/
Go straight		/	/	-	-	/	/	/	/
Turn right		/	/	+	-	/	/	/	/
PTO start		/	/	/	/	/	/	+	-
Fast motion		/	/	/	/	/	/	-	+

In the manual control module, SB2 and SB4 are two-position rocker-type selection switches with the power supply holding function. The switch SB2 is used to control the stop, forward and backward of the chassis, and the switch SB4 is used to control the PTO start, stop and walk at high velocity. Furthermore, SB3 is a two-position rocker-type selector switch with a median disconnection and an automatic reset function. It is used to control the left turning, straight-line running and right turning of the chassis. SB5 is a switch with holding function, which is used to control the chassis four-wheel drive and two-wheel drive.

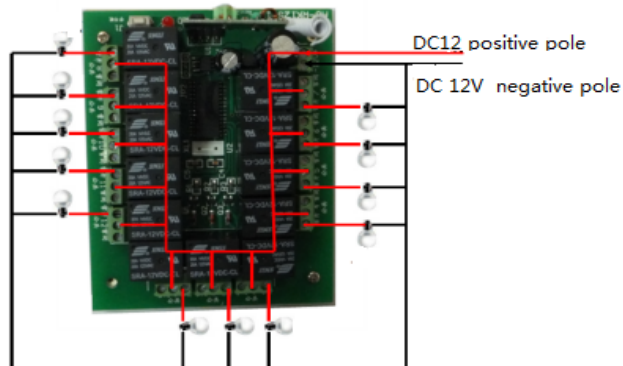


Fig. 5 Wireless remote receiving module

The principle is as follows:

When SB2 is in the neutral position, the chassis is stopped; when SB2 reaches the gearKM2, KM2 is powered on, and the normally open contacts are closed. 1YA is powered on, and the chassis is in a forward state.

When SB2 reaches KM3, KM3 is powered on, and the normally open contacts are closed. 2YA is powered on, and the chassis is in a backward state.

When SB4 is in the neutral position, the PTO system is stopped.

When SB2 reaches KM4, KM4 is powered on, and the normally open contacts are closed. 7YA is powered on, and the PTO system is started.

When SB4 reaches KM5, KM5 is powered on, and the normally open contacts are closed. 8YA is powered on, and the chassis is in a fast-running state.

When SB3 is in the middle position, both KM4 and KM5 are powered off, and the chassis is in a straight state.

When SB3 reaches KM4, KM4 is powered on, and the normally open contact of KM4 is closed. 3YA is powered on; the left wheel motor stops running, and the chassis starts to turn left.

When SB4 reaches KM5, KM5 is powered on, and the normally open contact of KM5 is closed. 4YA is powered on, the motor of the right wheel of the chassis stops rotating, and the chassis starts to turn right.

When SB5 is closed and KM6 is powered, its normally open contact is closed, and 5YA and 6YA are powered at the same time. At this time, the left and right rear wheel motors have no driving oil entering, i.e., the following state maintains, and the chassis is the front part of the two wheels.

When SB5 is powered off, KM6 would also be powered off. The left and right rear wheel motors have driving oil entering, and the chassis is in a four-wheel driving state.

The wireless remote control module contains transmitting and receiving ends and performs point-to-point transmission at a high wireless frequency of 315 MHz or 433.92 MHz [14-16]. The schematic diagram of the transmitting and receiving ends is shown in Fig. 5. The relay and power supply of the receiving device are 12-V DC power supplies, and the connected load is a contact relay to control the electromagnetic valve. There are 12 channels of buttons on the remote controller. Pressing key 1 on the remote controller will close A1 relay. When released, A1 relay will open. All relays have the same working mode, and only one channel of the relay can be active at a time. Therefore, the buttons on the remote controller of the transmitter can be regarded as an inching switch SY. The chassis can be controlled by the presented control circuit.

4. Results and Discussion

The proposed system is verified experimentally using a front axle swing steering test platform, swing walking chassis, belt, throttle opening control device, a tachometer, Shenzhen Renault CHPM460 portable hydraulic test equipment, and a PTT150 pressure sensor. The digital camera (model: Canon A590), a 15-V power supply, and eight parallel data lines. An accelerator control device was

installed on the chassis to keep the engine driving the oil pump at a constant output speed, so that the speed of the chassis could be maintained at the same level when driving in a straight line. The speed testers were installed on the sides of the four driving wheels to ensure that the speed of the chassis were consistent. A hydraulic pressure sensor was installed at the output end of each hydraulic motor. Under different load conditions, through the pressure gauge installed at the outlet of the control element and the speed measurement during the forward process, the pressure and flow of the system are measured to analyze the change of the input pressure of the chassis hydraulic motor during the steering process.

The watermark method is mainly used in the experiment of chassis linear driving. As shown in Fig.6, the chassis has straight driving required by the design and is not affected by the chassis load. This indicates that the hydraulic drive and its control system proposed in this paper can realize the expected driving conditions. Under smooth road conditions, the chassis can achieve high straightness with a deviation rate of less than 1%.

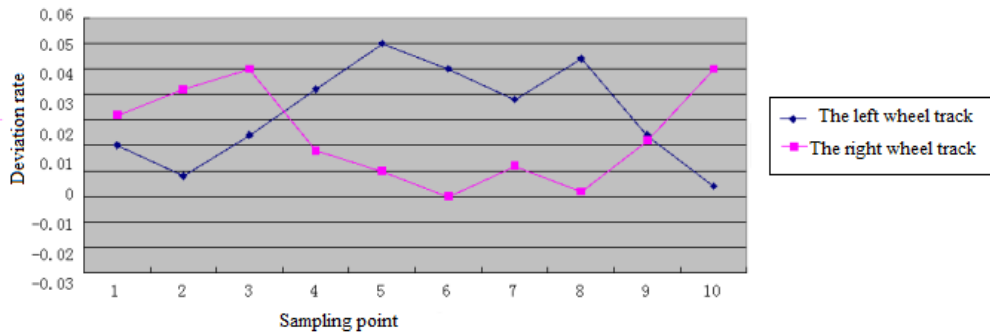


Fig.6 Travel straightness diagram

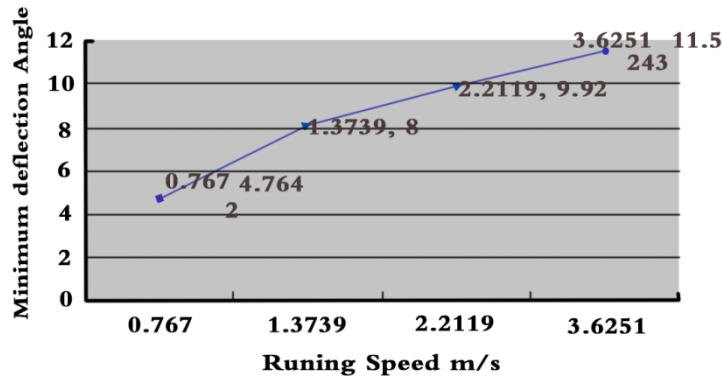


Fig.7 The relation between the minimum deflections

The steering angle test of the chassis mainly uses the electronic control. In this experiment, the steering is controlled by resetting the rocker switch. When the retractable rocker switch is moved to the left, the electromagnet of the hydraulic reversing valve connected with the left front wheel is electric, and the left front wheel loses power. Then the chassis begins to turn to the left, and the operation of the right steering is the same as the left turn. The minimum swing angle is related to the response speed of the electrical components, the driving speed of the chassis and the length of time for manual operation. The watermark method is used to measure the minimum swing angle of the front axle relative to the frame. Fig.7 shows a quasilinear relationship between the minimum deflection angle and the running speed of the chassis. The running speed of the chassis increases with the increase of the minimum deflection angle. At a driving speed of 0.767m/s, the minimum deflection angle was 4.764°. When the driving speed was 3.625m/s, the maximum value of deflection was 11.524°.

The engine always works at the same throttle opening when the chassis is set to drive in different conditions. The CHPM handheld tester is used to collect the dynamic changes of the input pressure and input flow of each motor. Fig.8 shows the measured pressure of each motor. When the chassis runs with the dual-pumpoil, the pressure of the four motors rapidly rises from zero to peak after 0.5 s. At the maximum peak pressure of the right front wheel, the pressure of the left and right rear wheels was 4.6 MPa, and the peak pressure of the left front wheel was 9.0 MPa. After 2.5 s, a stable running state was reached. At this time, the input pressures of the rear axle two-wheel motor, the left front wheel motor, and the right front wheel motor fluctuated within the range of 1.1 MPa, 1.5 MPa and 1.0 MPa respectively. The pressure difference between the input and output of the left front wheel motor fluctuated within the range of 0.6 MPa, and the pressure change of all four motors tended to be consistent.

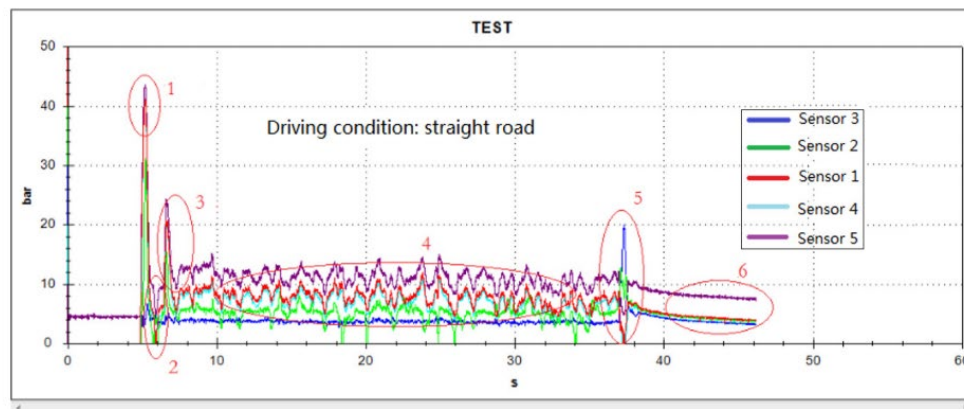


Fig.8 Pressure data of each motor

5. Conclusions

In this paper, an electro-hydraulic control system is adopted for the front axle swing steering chassis. According to the actual working condition of the chassis, the electric control system that can be operated manually or automatically is selected. The steering function of the chassis should meet the different speed requirements of the left and right motors to control the power-on/off of the electromagnetic reversing valve, so as to realize the steering of the front wheels. When the oil circuit of the reversing valve on one side is open and that on the other side is closed, the speed of the left and right travelling wheels will be different. In this paper, a relay contact electrical control scheme is used to establish an electro-hydraulic control system without considering the influence of energy consumption. The electrical control system includes a reversing circuit, a flow control, and a lifting position locking circuit. The straight-line and steering trajectories of the chassis were obtained by using the watermark method. When walking, the chassis can steer at a small angle to realize the steering of the chassis. The minimum deflection angle of the chassis is approximately linear to the driving speed. With the increase of the driving speed of the chassis, the minimum deflection angle will also increase.

An experimental evaluation of the controlled system was carried out. The pressure test results of the motors of the chassis show that when driving in a straight line, the pressure difference between the motors is controlled at 0.6MPa; during the steering process, the pressure change is also within the allowable range, which proves that the chassis can run stably.

Acknowledgements

This key project is supported by the Special Research Project on the Key Fields in General Universities of Guangdong Province (Grant nos. 2020ZDZX2033); Guangdong Province Science and Technology Innovation New Strategy Special Project (2018B010204); Lingnan Normal University Talent Project (ZL2023).

R E F E R E N C E S

- [1] *Luo, X.W.*, Thoughts on Accelerating the Development of Agricultural Mechanization in China. *Agriculture Engineering*, vol. 1, no. 4, pp. 1-8+56, 2011.
- [2] *Wang, S.S., Geng, L.X.*, Development Situation and Countermeasures of Agricultural Mechanization in Hilly and Mountain Areas. *Agriculture Engineering*, vol. 6, no. 5, pp. 1-4, 2016.
- [3] *Park, G., Han, K., Nam, K., Kim, H., Choi, S.B.*, Torque vectoring algorithm of electronic-four-wheel drive vehicles for enhancement of cornering performance. *IEEE*

Transactions on Vehicular Technology, vol. 69, no. 4, pp. 3668-3679, 2020. DOI: 10.1109/TVT.2020.2978099

- [4] Song, Y., Shu, H., Chen, X., Luo, S., Direct-yaw-moment control of four-wheel-drive electrical vehicle based on lateral tyre-road forces and sideslip angle observer. IET Intelligent Transport Systems, vol. 13, no. 2, pp. 303-312, 2019. <https://doi.org/10.1049/iet-its.2018.5159>
- [5] Zeng, A.P., Qiu, X.L., Zhao, N., Li, Z.W., Design of Hydraulic Rear Wheel Drive Light Farm Machinery Paddy Field Self-propelled Chassis. Journal of Agricultural Mechanization Research, vol. 32, no. 7, pp. 149-151+159, 2010.
- [6] Zhang, L.X., Liu, S.R., Mao, E.R., Xie, B., Li, F.Q., Reliability analysis of agricultural machinery chassis drive axle housing based on ANSYS. Transactions of the Chinese Society of Agricultural Engineering, vol. 29, no. 2, pp. 37-44+294, 2013.
- [7] Wu, X., Design of Front Axle Swing the Steering-Wheel-Drive Chassis Hydraulic System. Guangzhou: South China Agricultural University, 2014.
- [8] Kim, S., Park, K., Song, H.J., Hwang, Y.K., Moon, S.J., Ahn, H.S., & Tomizuka, M., Development of control logic for hydraulic active roll control system. International Journal of Automotive Technology, vol. 13, no. 1, pp. 87-95, 2012. <https://doi.org/10.1007/s12239-012-0008-5>
- [9] Lan, J., Feng, Y., Li, X.Y., Wang, C.Y., Lu, C.L., Li, D.G., Design of Automatic Mechanical Endurance Test System for Circuit Breaker Handcart. High Voltage Apparatus, vol. 54, no. 12, pp. 18-23, 2018. DOI: 10.13296/j.1001-1609.hva.2018.12.004
- [10] Zhang, L., Robust Analysis and Optimization Design of Double Front Axle Steering System. SAE International Journal of Passenger Cars-Mechanical Systems, vol. 7, no. 1, pp. 7-14, 2014. <https://doi.org/10.4271/2013-01-9124>
- [11] Song, S., Qu, J., Li, Y., Zhou, W., Guo, K., Fuzzy control method for a steering system consisting of a four-wheel individual steering and four-wheel individual drive electric chassis. Journal of Intelligent & Fuzzy Systems, vol. 31, no. 6, pp. 2941-2948, 2016. DOI: 10.3233/JIFS-169178
- [12] Tian, E., Guan, J., Sun, C., Gu, L., & Zhang, Y., A data-driven chassis coordination control strategy. IET Intelligent Transport Systems, vol. 15, no. 8, pp. 1006-1017, 2021. <https://doi.org/10.1049/itr2.12069>
- [13] Sun, X., Shi, Z., Cai, Y., Lei, G., Guo, Y., Zhu, J., Driving-cycle-oriented design optimization of a permanent magnet hub motor drive system for a four-wheel-drive electric vehicle. IEEE Transactions on Transportation Electrification, vol. 6, no. 3, pp. 1115-1125, 2020. DOI: 10.1109/TTE.2020.3009396
- [14] Sid, M. N., Becherif, M., Aboubou, A., & Benmouna, A., Power control techniques for fuel cell hybrid electric vehicles: A comparative study. Computers and Electrical Engineering, vol. 97, pp. 107602, 2022. <https://doi.org/10.1016/j.compeleceng.2021.107602>
- [15] Ding, N., Prasad, K., & Lie, T. T., Design of a hybrid energy management system using designed rule-based control strategy and genetic algorithm for the series-parallel plug-in hybrid electric vehicle. International Journal of Energy Research, vol. 45, no. 2, pp. 1627-1644, 2021. <https://doi.org/10.1002/er.5808>
- [16] Xiao, G., Chen, Q., Xiao, P., Zhang, L., & Rong, Q., Multiobjective Optimization for a Li-Ion Battery and Supercapacitor Hybrid Energy Storage Electric Vehicle. Energies, vol. 15, no. 8, pp. 2821, 2022. <https://doi.org/10.3390/en15082821>.
- [17] Hang, P., Chen, X., Towards autonomous driving: Review and perspectives on configuration and control of four-wheel independent drive/steering electric vehicles, Actuators, vol. 10, no. 8, pp. 184, 2021. <https://doi.org/10.3390/act10080184>